Available online at www.sciencedirect.com
ScienceDirect
Journal of Hazardous Materials 150 (2008) 573–581
Journal of Hazardous Materials
www.elsevier.com/locate/jhazmat

Comparison and evaluation of methods for the determination of flammability limits, applied to methane/hydrogen/air mixtures

F. Van den Schoor [a,*], R.T.E. Hermanns [b], J.A. van Oijen [b], F. Verplaetsen [c], L.P.H. de Goey [b]

[a] *Katholieke Universiteit Leuven, Department of Mechanical Engineering, Celestijnenlaan 300A, 3001 Heverlee, Leuven, Belgium*
[b] *Eindhoven University of Technology, Department of Mechanical Engineering, P.O. Box 513, 5600 MB Eindhoven, The Netherlands*
[c] *Adinex N.V., Brouwerijstraat 5/3, 2200 Herentals, Belgium*

Received 5 February 2007; received in revised form 30 April 2007; accepted 4 May 2007
Available online 10 May 2007

Abstract

Different methods, both experimental and numerical, to determine the flammability limits are compared and evaluated, exemplified by a determination of the flammability limits of methane/hydrogen/air mixtures for hydrogen fuel molar fractions of 0, 0.2, 0.4 and 0.6, at atmospheric pressure and ambient temperature. Two different experimental methods are used. The first method uses a glass tube with visual observation of the flame, whereas the second method uses a closed spherical vessel with a pressure rise criterion to determine whether flame propagation has occurred. In addition to these experiments, the flammability limits are determined numerically. Unsteady planar and spherically expanding flames are calculated with a one-dimensional flame code with the inclusion of radiation heat loss in the optically thin limit. Comparison of the experimental results with the results of the planar flame calculations shows large differences, especially for lean mixtures. These differences increase with increasing hydrogen content in the fuel. Better agreement with the experimental results is found for the spherically expanding flame calculations. A limiting burning velocity of 5 cm/s is found to predict the upper flammability limit determined with the tube method very well, whereas the limiting flame temperature approach was found to give poorer agreement. Further analysis indicates that the neglect of flame front instabilities is the probable cause of the large differences between experimental and numerical results at the lower flammability limit.

Keywords: Flammability limits; Methane; Hydrogen

1. Introduction

Knowledge of the flammability limits of gaseous mixtures is important for the safe and economic operation of many industrial processes. There are several standardised experimental methods available to determine these limits [1–4]. These experiments are, however, cumbersome and time-consuming, especially at the elevated conditions of temperature and pressure at which many industrial processes are operated. Nowadays, the ever increasing computational capabilities together with the development of detailed reaction mechanisms have made the numerical computation of flames possible for a number of geometries, such as freely propagating flames, burner stabilised flames and counterflow flames. This has led to a number of studies in which the limits of flammability have been determined numerically. These include the simulation of one-dimensional (1D) planar [5,6] and quasi-1D spherically symmetric [7] freely propagating flames with the inclusion of a radiation heat loss term in the energy conservation equation and the application of a limiting burning velocity [8] or of a limiting flame temperature [9,10] below which flames are unable to propagate. A profound comparison and evaluation of these methods, however, was not found in literature. Therefore, the aim of this study is to evaluate these different methods. This evaluation will be based both upon a comparison of their intrinsic capabilities of capturing the different aspects of a near-limit flame relevant to its extinction, as upon a comparison of their results with experimental data. Two different experimental methods will be used to determine these data, one using a visual criterion and one using a pressure rise criterion to ascertain flame propagation. This will allow us to compare both experimental methods and to choose the most

* Corresponding author. Tel.: +32 16 32 25 49; fax: +32 16 32 29 85.
E-mail address: Filip.VandenSchoor@mech.kuleuven.be (F. Van den Schoor).

0304-3894/$ – see front matter © 2007 Elsevier B.V. All rights reserved.
doi:10.1016/j.jhazmat.2007.05.006

appropriate one for the evaluation of the numerical methods. The scope of this study will be limited to flames at atmospheric pressure and ambient temperature. Methane/hydrogen mixtures are chosen as fuel, since it is expected that they will present an adequate challenge for the different methods. Moreover, there exists renewed interest in hydrogen addition to natural gas as a possible means of reducing the emissions of CO and CO_2 in lean premixed combustion devices. For example, in the Netherlands, government considers adding hydrogen to the natural gas grid, which feeds all household burners, making the results of this study highly relevant.

2. Experimental methods

The mixtures to be tested are prepared by mixing the separate flows coming from two thermal mass flow controllers, one for the methane/hydrogen mixture and one for air. The methane/hydrogen mixtures are acquired in high pressure cylinders. Analysis of the three different methane/hydrogen mixtures used in this study gives hydrogen concentrations of 20.0 ± 0.4 mol%, 40.3 ± 0.8 mol% and 59.9 ± 0.8 mol%, respectively. The lower flammability limit (LFL) is taken as the concentration of a non flammable mixture for which a 0.2 mol% richer mixture is flammable, whereas the upper flammability limit (UFL) is taken as the concentration of a non flammable mixture for which a 0.2 mol% leaner mixture is flammable. Gas chromatography is used at regular intervals to verify the mixture composition. The test mixtures are prepared with a maximum uncertainty of 0.2 mol% on the fuel fraction, giving an equal uncertainty on the flammability limit.

The first apparatus is based upon the German DIN 51649 standard [1]. It consists of a 300 mm long cylindrical tube with an inner diameter of 60 mm, which is placed vertically. The tube is made of glass so that the flame behaviour can be observed visually. This set-up uses a spark discharge between two electrodes placed 60 mm above the bottom of the tube as ignition source. Adopting the new European standard EN 1839 [2] the spark discharge time is 0.2 s, giving an ignition energy of approximately 2 J. A visual flammability criterion is used: flame propagation is said to have occurred if the flame detaches from the electrodes and propagates a distance of at least 100 mm.

The second apparatus is a spherical explosion vessel with an internal diameter of 200 mm (internal volume of 4.2 l). The pressure evolution after ignition is measured with a Kistler 701A piezoelectric pressure transducer. Ignition of the test mixtures is achieved by fusing a coiled tungsten wire, placed at the centre of the vessel, by applying a voltage of 40 V dc. The igniter releases about 10 J in 40 ms, independently of pressure or temperature. A pressure rise criterion is used to determine the flammability limit: flame propagation is said to have occurred if ignition is followed by a pressure rise of at least 5% of the initial pressure.

Further details about the experimental set-up and procedure can be found elsewhere [11]. All experiments are performed at an initial pressure of 102 ± 1 kPa and an initial temperature of 295 ± 3 K.

3. Numerical methods

The numerical calculations are performed using CHEM1D [12], a one-dimensional (1D) flame code capable of solving 1D mass, energy and species conservation equations with detailed transport and chemical kinetics models. Two different flame geometries are used, namely 1D planar premixed flames, both steady and unsteady, and quasi 1D spherically expanding premixed flames. The density, the temperature and the species mass fractions are specified at the cold boundary, while vanishing gradients are imposed at the hot boundary. Further details about the flame code can be found elsewhere [13].

Since for the atmospheric methane/hydrogen/air mixtures under investigation the Planck mean absorption length is of the order of one metre, reabsorption is unimportant in the experimental equipment used in this study [6]. Therefore, radiation heat loss is modelled by means of the optically thin limit. Four radiating species are considered, namely CO_2, H_2O, CO, and CH_4.

Two different chemical mechanisms are used to calculate the methane/hydrogen/air flames: the GRI 3.0 mechanism [14] which contains 325 elementary reactions and 53 species and the Smooke mechanism [15] which contains only 25 elementary reactions and 16 species. The GRI 3.0 mechanism was optimised for methane and natural gas as a fuel and can be used for both lean and rich flame calculations. The Smooke mechanism, however, cannot be used to calculate rich flames, since it only includes C_1-chemistry.

The flammability limits for the planar flames are determined by considering whether an unsteady flame calculation reaches a steady state or not. In the latter case, the maximum flame temperature and burning velocity will decrease continuously in time [5]. Before doing unsteady flame calculations, an initial guess for the lower (upper) flammability limit is sought by carrying out a series of steady flame calculations in which the equivalence ratio is decreased (increased) in steps of 0.001 until a steady solution cannot be found upon a further decrease (increase) of the equivalence ratio. Next, steady solutions in the neighbourhood of this initial guess are calculated with only 90% of the total radiation heat loss included. Because of the smaller heat loss, steady solutions can be found for leaner (richer) mixtures. Finally, these solutions serve as initial conditions for the unsteady calculations, which are done from their start with the radiation heat loss restored to the full 100%.

In the spherical flame calculations, the gas mixture is ignited by means of a source term in the energy conservation equation. This ignition source is modelled as an energy input of 2.1 J during a period of 200 ms in a spherical volume with a diameter of 5 mm. These parameters are chosen to resemble the ignition source that is used in the tube experiments, which is an electrostatic spark, releasing approximately 2 J in 200 ms between two electrodes placed 5 mm apart. Since spherical flame calculations with the GRI 3.0 mechanism are time-consuming, the Smooke mechanism is used to reduce the computational times for flames near the lean flammability limit. Mixtures in which flames propagate over a distance of 100 mm, are considered to be flammable, even if they extinguish at larger distances from the

ignition source. This definition was adopted to enable optimal comparison with the experimentally determined values. Due to the large computational time and the absence of a good initial guess for the flammability limit, the equivalence ratio at which calculations are performed is changed in steps of 0.01 for lean mixtures and of 0.1 for rich mixtures.

The planar flame calculations with the inclusion of the radiation heat loss term in the energy conservation equation (unless stated otherwise) will also be used to determine values for the burning velocities and the maximum flame temperatures which enable evaluation of the limiting burning velocity and limiting flame temperature approaches.

It is difficult to ascertain the uncertainty in the numerical calculations caused by uncertainties in the reaction rate parameters, in the transport properties, etc. The comparison and the evaluation of the different numerical methods is, however, not biased by any modelling uncertainty.

4. Theoretical background

In Section 5 the outcome of the different numerical methods will be evaluated based upon a comparison with experimental data. Here, however, we will evaluate them a priori based upon their intrinsic capabilities of capturing the different aspects of a near-limit flame that are relevant to its extinction. Table 1 gives an overview of these flame aspects, together with the required geometry of the numerical model to capture them. Obviously, the simplest geometry to study flame propagation is that of a 1D planar freely propagating flame. However, to study flame extinction a loss term must be introduced into the flame equations [16]. Since flames will always lose part of their energy by radiation heat transfer [6], the most straightforward approach is introducing a radiation heat loss term into the energy conservation equation [5,6]. This is, thus, the simplest numerical method to determine the flammability limits, since it only uses a 1D planar geometry. The flames that occur in the experimental determination of the flammability limits (see Section 2), are, however, far from planar. Upon ignition a flame kernel is formed, which spreads out spherically. At the same time it starts to rise as a result of natural convection. This causes the flame to become stretched due to two separate effects, namely its spherical expansion and its interaction with the flow field caused by its buoyancy. This flame stretch needs to be taken into account to accurately calculate flammability limits. The effect of the flame curvature induced by the outward expansion of the flame, can be investigated by doing flame calculations in a quasi 1D spherically symmetric geometry [7]. These calculations, however, only include part of the flame stretch—especially the stretch in the early development of the flame kernel immediately after ignition. Allowing for the total flame stretch would require the calculation of the entire flow field, induced by natural convection. The simplest geometry that enables such a calculation is a quasi-two-dimensional (2D) axisymmetric one with the symmetry axis parallel to the gravitational acceleration vector. The numerical calculation of the complete interaction between the flame front and the flow field that it induces, is, however, hardly feasible when using detailed chemical kinetics models. As a result, the direct numerical calculation of flammability limits is restricted to 1D planar and quasi 1D spherical freely propagating flames. For the calculation of flammability limits in a zero-gravity environment the calculation of spherically expanding flames might be sufficient. When calculating the limits in a normal 1 g environment, however, it must be borne in mind that neither natural convection, nor flame front instabilities are taken into account by these flame calculations.

Table 1
Overview of the flame aspects relevant to the calculation of flammability limits together with the required geometry of the numerical model

Flame aspects	Geometry of numerical model
Reaction kinetics	1D planar
Heat loss	1D planar
Flame curvature	Quasi-1D spherically symmetric
Natural convection	Quasi-2D axisymmetric
Flame front instabilities	3D

Yet, there exists an approximate method to include the effect of the flame stretch caused by natural convection. By equating the stretch experienced by a flame propagating upwards in a cylindrical tube with the stretch necessary to extinguish the flame, Buckmaster and Mikolaitis [17] derived an expression for the burning velocity, below which flames are unable to propagate. The application of a limiting burning velocity is, thus, not solely empirically based, as suggested by Westbrook [18], but it can also be derived theoretically, thereby also exhibiting its pressure and temperature dependence [17,19]. Since it takes into account natural convection, albeit approximately, it is expected to give a better agreement with the experimental results than the planar or spherical flame calculations.

Analogous to the concept of a limiting burning velocity, is that of a limiting flame temperature. It is based upon the empirical finding that the heat liberated by a mole of lean limit mixtures is nearly constant for many hydrocarbon/air mixtures [20,21], implying that the adiabatic flame temperature at the lower flammability limit should also be nearly constant. This approach is often used when predicting the flammability limits of fuel/air/diluent mixtures, based upon the limits for the fuel/air mixture [9,10]. It is also implicitly used when applying Le Chatelier's mixing rule, since this rule is based upon the assumption that the heat of combustion of the combustible mixture at the (lower) flammability limit is constant, equalling the heat of combustion of the composing combustibles at their respective (lower) flammability limits [22]. Since the application of a constant limiting flame temperature is solely based upon experimental data at the lower flammability limit, it might result in poor agreement between calculated and experimental results, especially at the upper flammability limit.

An important aspect of flame propagation that is not taken into account in any of the above-mentioned methods are flame front instabilities. Therefore, it is likely that whenever these instabilities are present, none of the methods will yield satisfactory results. Only 3D numerical calculations can reveal these effects.

Table 2
Experimentally determined flammability limits of methane/hydrogen/air mixtures

Fuel composition		LFL				UFL			
CH_4 (mol%)	H_2 (mol%)	Tube		Bomb		Tube		Bomb	
		mol%	ϕ	(mol%)	ϕ	(mol%)	ϕ	(mol%)	ϕ
100	0	4.4	0.438	4.6	0.459	15.8	1.787	16.0	1.814
80	20	4.2	0.355	4.4	0.373	19.0	1.899	19.6	1.973
60	40	4.0	0.278	4.6	0.321	24.2	2.128	25.4	2.270
40	60	4.0	0.218	4.6	0.253	32.4	2.511	–	–

5. Results

5.1. Experimental results

The flammability limits were determined experimentally with two different methods: the tube method and the bomb method. Table 2 shows the results of the experiments. It can be seen that an increase in the hydrogen content of the fuel widens the flammable range expressed in terms of the equivalence ratio ϕ: it lowers the LFL and raises the UFL. The UFL could not be determined for mixtures with a methane/hydrogen molar ratio of 40/60 using the bomb method due to experimental difficulties. The higher thermal conductivity of these mixtures caused a large variance on the ignition energy, since the tungsten wire did not always fuse during ignition.

When comparing the results from both methods it can be seen that there are differences of more than 0.2 mol%, meaning that they are significant. Since all tests were repeated with a single mixture used in both experimental set-ups, it was concluded that the different flammability limit values were not caused by differences in mixture composition. As the largest disparity between the two methods is the use of a different flammability criterion, its effect on the experimental results was investigated. Since the spherical explosion vessel does not allow visual observation of the flame, the bomb method uses an indirect measurement of the flame propagation, namely the ensuing pressure increase. It is, thus, incapable of clearly distinguishing between local burning in the vicinity of the ignition source and flame propagation over a certain distance. Therefore, an other criterion was required to determine whether or not the flame was propagating away from the ignition source, allowing a better comparison with the experimental results of the tube method. Based upon the knowledge that lowering the ignition source leads to higher explosion pressures if the mixture supports flame propagation [23], a new method was devised. Two series of tests were done, one with central ignition and the other with the ignition source lowered by 40 mm. A single mixture was prepared for the experiments at both ignition source locations to ensure that the mixture composition was the same. By comparing the results of both test series, it was possible to better distinguish between flame propagation with low pressure rise and local burning.

Fig. 1a shows the results at the lean side for a mixture with a methane/hydrogen molar ratio of 60/40. Mixtures of 4.4 mol% and 4.6 mol% fuel were tested, which are just inside the flammable range determined with the tube method. They show flame propagation over the entire length of the glass tube. They are, however, found to be non-flammable when using the bomb method. It is found that lowering the ignition source leads to a slight increase in explosion pressure. Thus, these flames might also support flame propagation inside the closed spherical vessel, albeit with a very small pressure increase. Fig. 1b shows the results at the rich side for a mixture with pure methane as fuel. Mixtures of 15.6 mol% and 15.8 mol% methane were tested, which are, respectively, just inside and outside the flammable range determined with the tube method. It is found that experiments at 15.6 mol% methane, give a large difference in pressure increase between the central and the lowered ignition source position. The experiments at 15.8 mol% methane, however, show an erratic behaviour with no clear trend. The observed

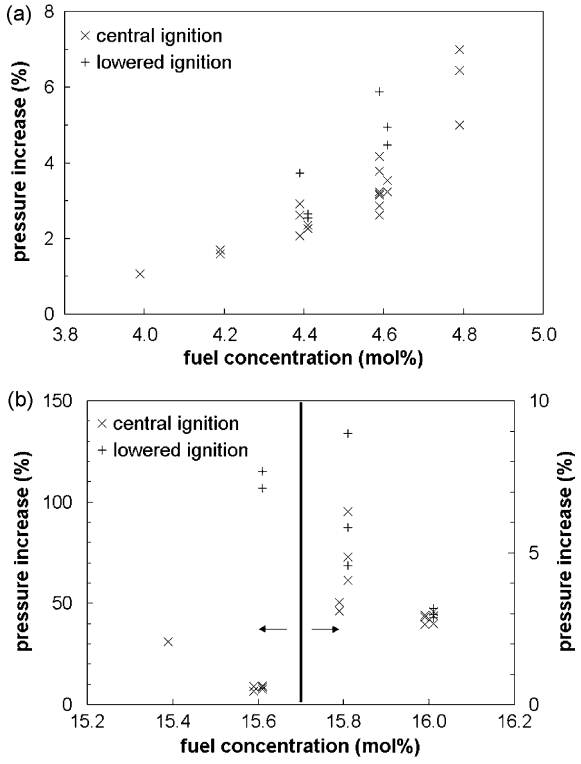

Fig. 1. Pressure increase expressed as a percentage of the initial pressure plotted against molar concentration of the fuel with the ignition source placed in the centre of the explosion vessel (central ignition) and at 40 mm below the centre (lowered ignition) for a methane/hydrogen/air mixture with a methane/hydrogen molar ratio of 60/40 (a) en for a methane/air mixture (b). Distinction is made between measurement points obtained from experiments with one single mixture ensuring constant fuel concentration (shifted to the right for clarity), and those obtained otherwise (shifted to the left).

scatter in the measured pressure increases reflects the stochastic nature of the ignition process near the flammability limits. Such a behaviour suggests that these mixtures do not support flame propagation, but merely burn locally near the ignition source. The findings of these additional experiments corroborate the idea that the difference between the results from both methods stems primarily from the different flammability criteria used. Moreover, the tube method is found to give results that can be more readily compared with those of the numerical calculations.

Similar discrepancies between the values of the flammability limits determined using different standards have been reported by De Smedt et al. [24] and by Razus et al. [25]. De Smedt et al. made a comparison between the flammability limits obtained with the DIN 51649 standard [1], which uses a visual criterion of flame detachment, and those obtained in a closed spherical vessel using a 7% pressure rise criterion. They found that DIN 51649 gave systematically wider limits and recommended the use of a 2% pressure rise criterion to bring the results of both methods in closer agreement. Razus et al. compared the data of De Smedt et al. with data obtained using the Bureau of Mines method [26], which requires flame propagation over a distance of at least 1.5 m to term a mixture flammable. They found that the Bureau of Mines method gave the narrowest limits. In conclusion, both these previous studies also emphasise the importance of the flammability criterion in the experimental determination of flammability limits.

Wierzba and Ale [27] have measured the UFL of methane/hydrogen/air mixtures in a cylindrical tube, with a diameter of 50.8 mm and a height of 1 m. Ignition was initiated by an electric spark discharge. The electrode gap and the spark duration were adjusted to give the widest flammable range. They, however, do not report values for these parameters, nor for the ignition energy. A mixture was considered flammable, if it supported flame propagation over the entire length of the tube. Gasse, as cited by Schröder [28], has determined the UFL of methane/hydrogen/air mixtures following the DIN 51649 [1] standard. Pahl, as cited by Schröder [28], has measured the LFL and UFL of methane/hydrogen/air mixtures in a closed cylindrical bomb, with a diameter of 150 mm and a height of 150 mm. Ignition was achieved by means of a fuse wire placed at the centre of the vessel, which released an ignition energy of approximately 40 J. Flame propagation was said to have occurred if ignition was followed by a pressure rise of at least 10% of the initial pressure. Fig. 2 shows a comparison between our experimental results and those of these researchers. The results of Gasse agree very well with those obtained in this study using the tube method. The use of a longer spark duration (0.5 s) and a less severe flammability criterion (flame detachment from the electrodes) explain why the limits found by Gasse are slightly wider than ours. Comparison of the results of this study obtained in the closed bomb with those of Pahl who used a similar experimental set-up shows differences of up to 3 mol%. The higher ignition energy used by Pahl could explain the wider limits even with the use of a more severe flammability criterion. The requirement of flame propagation over a length of 1 m, applied by Wierzba and Ale makes their flammability criterion much more severe than ours, giving rise to lower UFL's. Overall, there is good agreement between the experimental results at the UFL. At the LFL the differences between our results and those of Pahl are smaller than the experimental uncertainties.

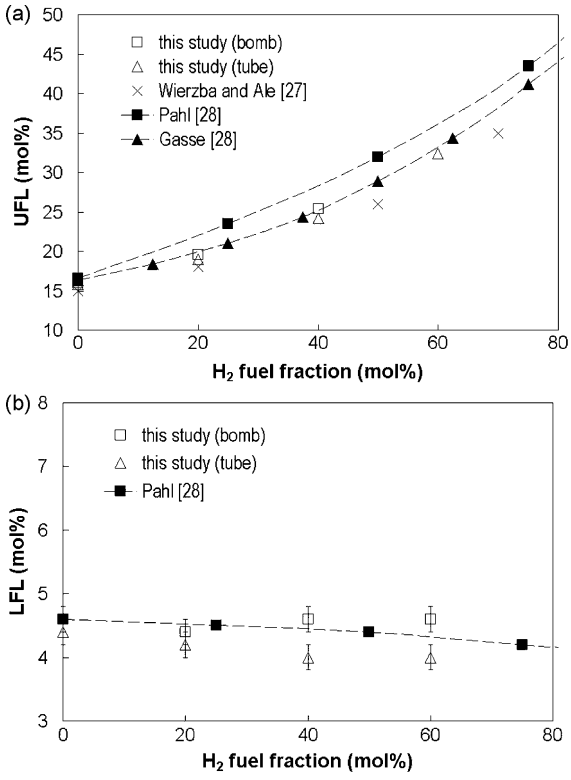

Fig. 2. Flammability limits of methane/hydrogen/air mixtures plotted against hydrogen fuel fraction.

5.2. Numerical results

Fig. 3 shows a comparison between the experimentally determined flammability limits and those calculated with the planar and spherical flame calculations. It can be seen that the results of the planar flame calculations differ substantially from the ones obtained experimentally. The difference is largest for lean mixtures and increases with increasing hydrogen content in the fuel. The results of the spherical flame calculations are in closer agreement with the experimental ones. This was expected, since these calculations include part of the flame stretch (see Section 4). The effect of this flame stretch is shown in Fig. 4 in which a spherical flame and a steady planar flame are compared for a lean ($\phi = 0.60$) and a rich ($\phi = 2.00$) mixture with a methane/hydrogen molar ratio of 40/60. For lean mixtures, the spherical flame has a maximum flame temperature of 1759 K, while the planar flame only reaches a temperature of 1700 K. Moreover, the spherical flame has a lower final oxygen concentration and higher overall radical concentrations. Both indicate that the spherical flame is more reactive than the planar flame causing the observed lowering of the calculated LFL (Fig. 3). This increased reactivity also leads to a higher burning velocity (see below). Opposite results are found at the UFL (Figs. 3 and 4).

Fig. 5 shows the propagation of a spherical flame with a methane/hydrogen molar ratio of 40/60 at different equivalence

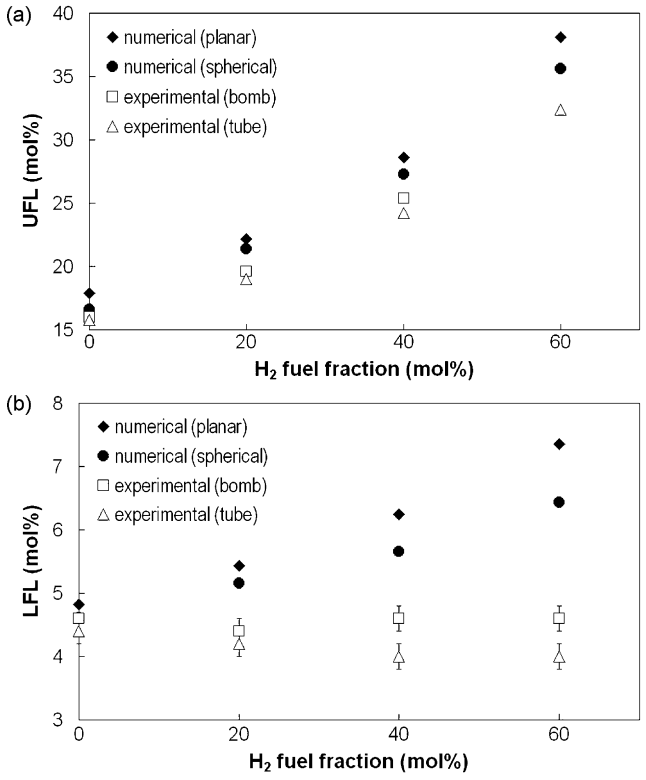

Fig. 3. Experimentally and numerically determined upper flammability limits (a) and lower flammability limits (b) of methane/hydrogen/air mixtures plotted against hydrogen fuel fraction.

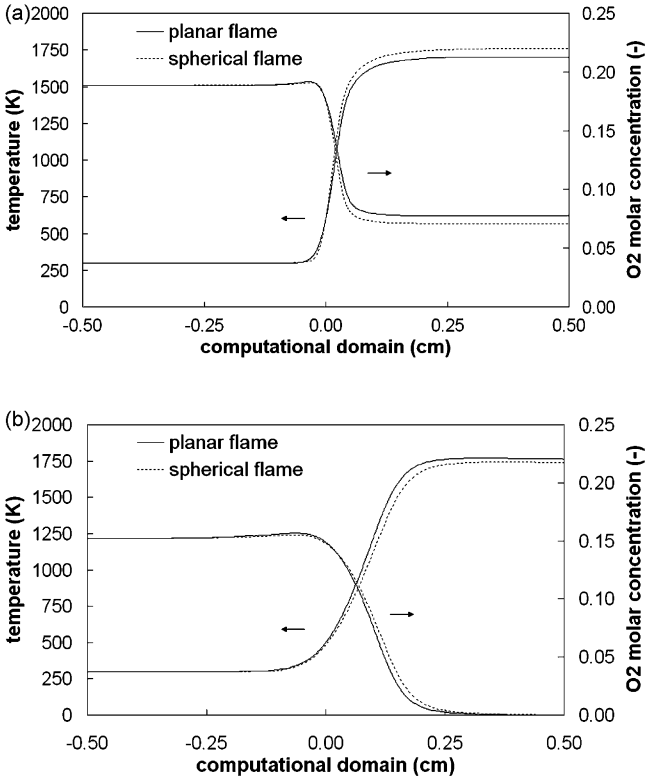

Fig. 4. Comparison between numerically calculated temperature and oxygen concentration profiles for a stationary planar and a spherically expanding methane/hydrogen/air flame with a methane/hydrogen molar ratio of 40/60 at an equivalence ratio $\phi = 0.60$ (a) and $\phi = 2.00$ (b).

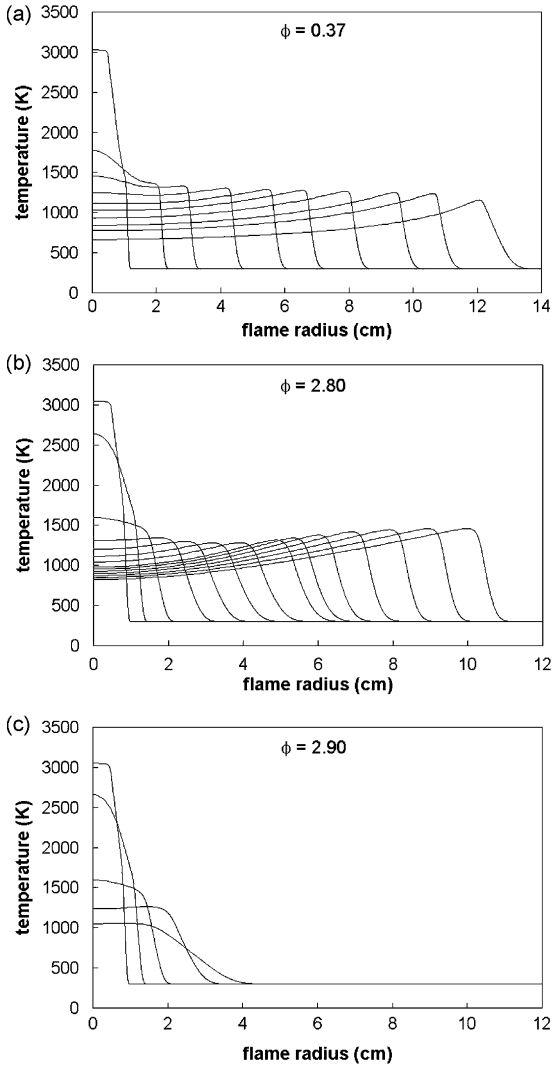

Fig. 5. Numerically calculated temperature profiles for a spherically expanding methane/hydrogen/air flame with a methane/hydrogen molar ratio of 40/60 at an equivalence ratio $\phi = 0.37$ (a), $\phi = 2.80$ (b) and $\phi = 2.90$ (c).

ratios. The mixture at $\phi = 0.37$ was termed flammable as the flame propagates over a distance of at least 100 mm. Nevertheless, the flame temperature continuously drops during flame propagation, eventually leading to extinction of the flame at a distance of approximately 120 mm. This is not surprising, since the flame stretch which leads to the increased flame temperature continuously decreases as the flame radius increases. This behaviour is observed experimentally at micro-gravity and is termed self-extinguishing flames [29]. For rich mixtures spherical flame propagation occurs with a continuously increasing flame temperature as the stretch decreases. As a result these flames will propagate indefinitely ($\phi = 2.80$) or they will extinguish immediately after they are initiated ($\phi = 2.90$).

The application of a limiting burning velocity and of a limiting flame temperature are shown in Figs. 6 and 7, respectively. A limiting burning velocity of approximately 5 cm/s is found to predict the upper flammability limit determined with the tube method very well (Fig. 6a). This value is in the range of theoretically derived [16,18] and experimentally determined [30]

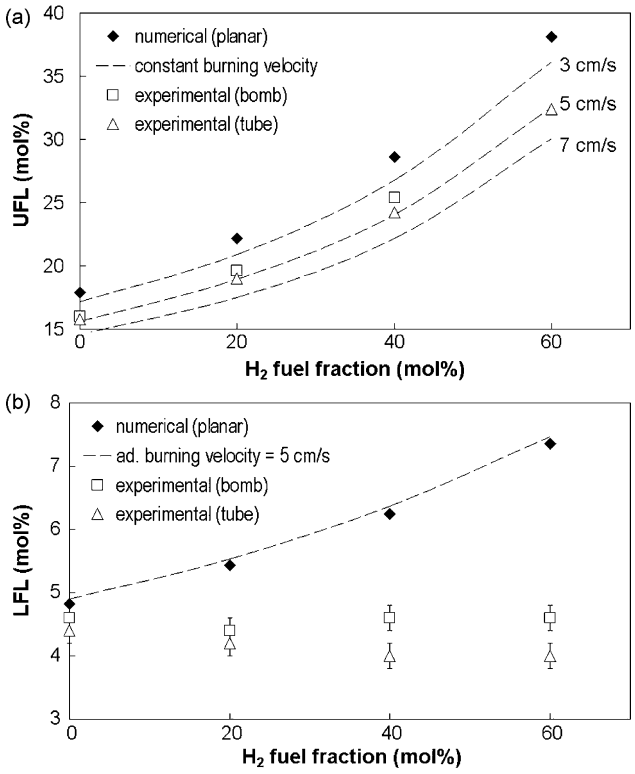

Fig. 6. Comparison of calculated burning velocities with experimentally determined upper flammability limits (a) and lower flammability limits (b) of methane/hydrogen/air mixtures plotted against hydrogen fuel fraction.

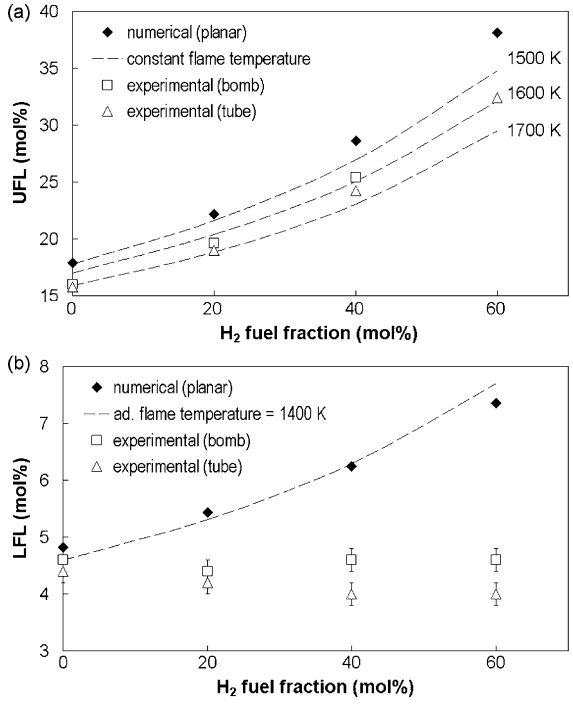

Fig. 7. Comparison of calculated flame temperatures with experimentally determined upper flammability limits (a) and lower flammability limits (b) of methane/hydrogen/air mixtures plotted against hydrogen fuel fraction.

values for the limiting burning velocity. As can be seen in Fig. 7a, the use of a limiting flame temperature gives a slightly worse agreement with the experimentally determined upper flammability limits than does that of a limiting burning velocity. This is expected since the constancy of the flame temperature was experimentally observed for mixtures at the lower flammability limit only (see Section 4). At the lower flammability limit, however, both methods show large differences with the experimental data (Figs. 6b and 7b). Since the experimentally determined LFL values are lower than those obtained with the (non-adiabatic) planar flame calculations, adiabatic planar flame calculations were necessary to obtain values of the adiabatic burning velocity and the adiabatic flame temperature at the LFL. Unrealistically low values are found for the limit adiabatic burning velocity (less than 1 cm/s), while the limit adiabatic flame temperature decreases from 1357 K for pure methane to 1078 K for a mixture with a methane/hydrogen molar ratio of 60/40.

It is believed that the unsatisfactory results for all methods at the lower flammability limit are caused by the omission of flame front instabilities, leading to the formation of cellular flame propagation, where the flame breaks up in individual cells. These cellular flames are highly susceptible for the effect of preferential diffusion of fuel and oxygen: the higher mass diffusivity of methane and especially that of hydrogen with respect to oxygen can make a flame behave as though it is actually richer [31]. The higher the hydrogen content in the fuel, the larger will be the impact of this phenomenon on the flame propagation, which explains the increasing difference with increasing hydrogen content (Figs. 3b, 6b and 7b). The breaking up of the flame could, however, not clearly be seen in the glass tube experiments. Still, this does not mean that cellular flame formation is absent, as the low luminosity of these hydrogen enriched flames and the rapidity of the phenomenon seriously complicate observations made with the naked eye. Moreover, there is some indirect experimental evidence. It was found that near the LFL flames propagate with a very small pressure increase, whereas flames near the UFL show very large pressure increases, especially if the ignition source is lowered (Section 5.1). This can be explained by the presence of cellular flame formation at the lean limit and its absence at the rich limit, since this phenomenon causes only part of the mixture to be actually traversed and consumed by the flame.

There is more evidence that the methane/hydrogen/air flames become unstable near the lean limit, especially for high hydrogen contents. The Markstein number Ma, governs the sensitivity of the burning velocity S_L to changes in flame stretch rate K by $S_L = S_L^0(1 - MaKa)$. In this expression, flame stretch rate K is quantified in terms of the Karlovitz number $Ka = K\delta_f/S_L^0$ with δ_f being the flame thickness and S_L^0 the unstretched burning velocity [32]. The Markstein number is a measure to quantify the sustainability of flames to instabilities. Flames are stable if the Markstein number is positive and unstable if it is negative, leading to cell formation during flame propagation. The Markstein numbers are determined for different equivalence ratios and different hydrogen fuel fractions by solving the 1D equations for weakly stretched planar flames [33]. Fig. 8 shows the results of these calculations for lean flames

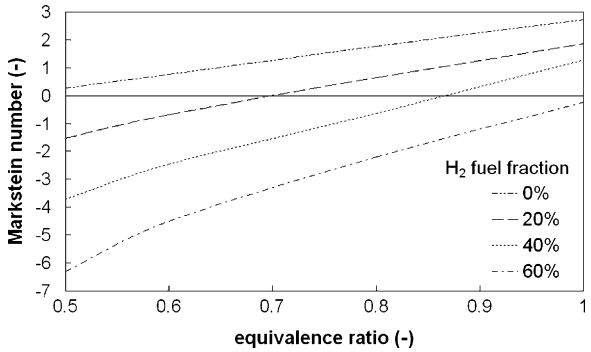

Fig. 8. Numerically calculated Markstein numbers of weakly stretched planar methane/hydrogen/air flames plotted against equivalence ratio for different hydrogen fuel fractions.

using the Smooke mechanism. Note that the Markstein number decreases for decreasing equivalence ratio and increasing hydrogen fuel fraction. These results indicate that the flames are unstable near the lean limit. The flames become more unstable if the hydrogen fuel fraction is increased. Recent experiments in methane/air flames [34] and methane/hydrogen/air flames [32,35] have shown a similar behaviour for the Markstein number. Huang et al. [35] also concluded from their measurements that lean methane/hydrogen/air flames are unstable, while lean methane flames and rich methane/hydrogen/air flames are stable. This flame instability, thus, explains the increasing deviation between numerical and experimental results for increasing hydrogen content in the mixture at the LFL.

6. Discussion

Both the theory (Section 4) and the comparison of experimental and numerical results (Section 5.2) indicate that in the absence of flame front instabilities, the application of a limiting burning velocity has the best potential for accurately calculating the flammability limits. It must be noted, however, that a constant limiting burning velocity can only be used at constant pressure and temperature, as was the case in this study. This limitation follows from the theoretical derivation of the limiting burning velocity, which allows for its pressure and temperature dependence [16,18]. If an accurate value for the flammability limits is not required, but only a safe value, i.e. lower (higher) than the experimental LFL (UFL), the calculation of planar or spherical flames with the inclusion of a radiation heat loss term in the energy conservation equation is sufficient, again, however, requiring the absence of flame front instabilities. On the contrary, if flame front instabilities are present, none of the studied methods gives satisfactory results, as expected from the theoretical background (Section 4). As a result, when calculating flammability limits, it is important to know whether the mixture is prone to flame front instabilities. As already mentioned in Section 5.2, the stability of a flame is governed by the Markstein number *Ma*: if *Ma* is negative the flame is unstable. For a two-reactant mixture and a single-step reaction, Clavin and Williams [36] found that if the Lewis number $Le = \alpha/D$, with α the thermal diffusivity of the mixture and D the mass diffusion coefficient of the deficient reactant, is larger than 1, the Markstein number will be positive. This result is not surprising, since it is the thermal-diffusive instability that destabilises the flame propagation at the limits. Since the Lewis number can be easily calculated, it can be used as an approximate measure of flame stability. In conclusion, if the Lewis number of one of the deficient components is smaller than 1, the flame could be unstable and care must be taken when using any of the methods studied in this paper to calculate the flammability limits.

7. Conclusions

Different methods for the calculation of flammability limits have been compared and evaluated. It is found that in the absence of flame front instabilities:

1. Planar flame calculations with the inclusion of radiation heat loss in the optically thin limit lead to safe, but inaccurate values for the flammability limits, due to the neglect of the effects of flame curvature and natural convection on limit flame propagation.
2. Spherical flame calculations with the inclusion of radiation heat loss in the optically thin limit show a marked improvement compared with the planar flame calculations, since they include part of the flame stretch, but still show a difference with the experimental values.
3. The application of a limiting burning velocity shows the best potential for calculating the flammability limits, since it takes natural convection into account, albeit approximately.
4. The application of a constant limiting flame temperature is less accurate than that of a limiting burning velocity.

If, however, flame front instabilities are present, none of the above-mentioned methods gives satisfactory results.

These conclusions are derived from a study of the flammability limits of methane/hydrogen/air mixtures, at atmospheric pressure and ambient temperature. To further corroborate them, future work will focus on the calculation of flammability limits at elevated pressures and temperatures.

References

[1] DIN 51649 Teil 1, Bestimmung der Explosionsgrenzen von Gasen und Gasgemischen in Luft, Deutsches Institut für Normung, Berlin, 1986.
[2] EN 1839, Determination of Explosion Limits of Gases and Vapours, European Committee for Standardisation, Brussels, 2003.
[3] ASTM E 918, Standard Practice for Determining Limits of Flammability of Chemicals at Elevated Temperature and Pressure, American Society for Testing and Materials, 1999.
[4] ASTM E 681, Standard Test Method for Concentration Limits of Flammability of Chemicals (Vapors and Gases), American Society for Testing and Materials, 1998.
[5] K.N. Lakshmisha, P.J. Paul, H.S. Mukunda, On the flammability limit and heat loss in flames with detailed chemistry, in: Proceedings of the 23rd Symposium on Combustion, The Combustion Institute, 1990, pp. 433–440.
[6] J. Yiguang, G. Masuya, P.D. Ronney, Effects of radiative emission and absorption on the propagation and extinction of premixed gas flames, in: Proceedings of the 27th Symposium on Combustion, The Combustion Institute, 1998, pp. 2619–2626.

[7] M. Sibulkin, A. Frendi, Prediction of flammability limit of an unconfined premixed gas in the absence of gravity, Combust. Flame 82 (1990) 334–345.
[8] M.N. Bui-Pham, J.S Miller, Rich methane/air flames: burning velocities, extinction limits, and flammability limit, in: Proceedings of the 25th Symposium on Combustion, The Combustion Institute, 1994, pp. 1309–1315.
[9] I. Wierzba, S.O. Bade Shrestha, G.A. Karim, An approach for predicting the flammability limits of fuel/diluent mixtures in air, J. I. Energy 69 (1996) 122–130.
[10] Y.N. Shebeko, W. Fan, I.A. Bolodian, V.Y. Navzenya, An analytical evaluation of flammability limits of gaseous mixtures of combustible-oxidizer-diluent, Fire Safety J. 37 (2002) 549–568.
[11] F. Van den Schoor, F. Verplaetsen, The upper explosion limit of lower alkanes and alkenes in air at elevated pressures and temperatures, J. Hazard. Mater. 128 (2006) 1–9.
[12] CHEM1D, A One-dimensional Laminar Flame Code, Eindhoven University of Technology. Available from: http://www.combustion.tue.nl/chem1d.
[13] B. Somers, The Simulation of Flat Flames with Detailed and Reduced Chemical Models, PhD thesis, Eindhoven University of Technology, 1994.
[14] G.P. Smith, D.M. Golden, M. Frenklach, N.W. Moriarty, B. Eiteneer, M. Goldenberg, C.T. Bowman, R. Hanson, S. Song, W.C. Gardiner Jr., V. Lissianski, Z. Qin, GRI 3.0. Available from: http://www.me.berkeley.edu/gri-mech.
[15] M.D. Smooke, V. Giovangigli, in: M.D. Smooke (Ed.), Reduced Kinetic Mechanisms and Asymptotic Approximations for Methane-Air Flames, Springer-Verlag, Berlin, 1999, pp. 1–28.
[16] K.N. Lakshmisha, P.J. Paul, N.K.S. Rajan, G. Goyal, H.S. Mukunda, Behavior of methane–oxygen–nitrogen mixtures near flammability limits, in: Proceedings of the 22nd Symposium on Combustion, The Combustion Institute, 1988, pp. 1573–1578.
[17] J. Buckmaster, D. Mikolaitis, A flammability-limit model for upward propagation through lean methane/air mixtures in a standard flammability tube, Combust. Flame 45 (1982) 109–119.
[18] C.K. Westbrook, Inhibition of hydrocarbon oxidation in laminar flames and detonations by halogenated compounds, Proc. Combust. Inst. 19 (1982) 127–142.
[19] P.D. Ronney, Understanding combustion processes through microgravity research, in: Proceedings of the 27th Symposium on Combustion, The Combustion Institute, 1998, pp. 2485–2506.
[20] H. Le Chatelier, O. Boudouard, Limits of flammability of combustible vapors, Compt. Rend. Acad. Sci. Paris 126 (1898) 1510–1513.
[21] M.J. Burgess, R.V. Wheeler, Lower limit of inflammation of paraffin hydrocarbons with air, J. Chem. Soc. 99 (1911) 2013–2030.
[22] H. Le Chatelier, O. Boudouard, Sur les limites d'inflammibilité des mélanges gazeux, Bull. Soc. Chim. Paris 19 (1898) 483–488.
[23] S. Crescitelli, G. Russo, V. Tufano, F. Napolitano, L. Tranchino, Flame propagation in closed vessels and flammability limits, Combust. Sci. Technol. 15 (1977) 201–212.
[24] G. De Smedt, F. de Corte, R. Notelé, J. Berghmans, Comparison of two standard test methods for determining explosion limits of gases at atmospheric conditions, J. Hazard. Mater. 70 (1999) 105–113.
[25] D. Razus, M. Molnarne, O. Fuss, Limiting oxygen concentration evaluation in flammable gaseous mixtures by means of calculated adiabatic flame temperatures, Chem. Eng. Process 43 (2004) 775–784.
[26] H.F. Coward, G.W. Jones, Limits of Flammability of Gases and Vapors, Bulletin 503, U.S. Bureau of Mines, Washington, DC, 1952.
[27] I. Wierzba, B.B. Ale, Rich flammability limits of fuel mixtures involving hydrogen at elevated temperatures, Int. J. Hydrogen Energy 25 (2000) 75–80.
[28] V. Schröder, Explosionsgrenzen von Wasserstoff und Wasserstoff/Methane-Gemischen, Forschungsbericht 253, Bundesantalt für Materialforschung und -prüfung, Berlin, 2002.
[29] P.D. Ronney, Effect of gravity on laminar premixed gas combustion. II. Ignition and extinction phenomena, Combust. Flame 62 (1985) 121–133.
[30] P.D. Ronney, H.Y. Wachman, Effect of gravity on laminar premixed gas combustion. I. Flammability limits and burning velocities, Combust. Flame 62 (1985) 107–119.
[31] G.H. Markstein, Nonsteady Flame Propagation, Bergamon Press, Oxford, 1964, pp. 9–12.
[32] F. Halter, C. Chauveau, N. Djebaïli-Chaumeix, I. Gökalp, Characterization of the effects of pressure and hydrogen concentration on laminar burning velocities of methane–hydrogen–air mixtures, in: Proceedings of the 30th Symposium on Combustion, The Combustion Institute, 2005, pp. 201–208.
[33] J.A.M. de Swart, G.R.A. Groot, J.A. van Oijen, J.H.M. ten Thije Boonkkamp, L.P.H. de Goey, Detailed analysis of the mass burning rate of stretched flames including preferential diffusion effects, Combust. Flame 145 (2006) 245–258.
[34] X.J. Gu, M.Z. Haq, M. Lawes, R. Woolley, Laminar burning velocity and Markstein lengths of methane–air mixtures, Combust. Flame 121 (2000) 41–58.
[35] Z. Huang, Y. Zhang, K. Zeng, B. Liu, Q. Wang, D. Jiang, Measurements of laminar burning velocities for natural gas–hydrogen–air mixtures, Combust. Flame 146 (2006) 302–311.
[36] P. Clavin, F.A. Williams, Effects of molecular diffusion and of thermal expansion on the structure and dynamics of premixed flames in turbulent flows of large scale and low intensity, J. Fluid Mech. 116 (1982) 251–282.